

Electro-Nanopatterning of Surface Relief Gratings on Azobenzene Layer-by-Layer Ultrathin Films by Current-Sensing Atomic Force Microscopy

Akira Baba, Guoqian Jiang, Kang-Min Park,[†] Jin-Young Park, Hoon-Kyu Shin,[†] and Rigoberto Advincula*

Department of Chemistry and Department of Chemical Engineering, University of Houston, 136 Fleming Building, Houston, Texas 77204-5003

Received: June 23, 2006; In Final Form: July 27, 2006

The electro-nanopatterning and mechanism of pattern formation in azobenzene-containing layer-by-layer (LbL) ultrathin films is described using surface probe microscopy techniques. First, arrays of nanodots were patterned on these films to investigate applied time at constant voltage bias dependence in electro-nanopatterning. The anisotropic mass transport and polar alignment of the azobenzene-containing films were observed after applying the electric field and heating the sample locally with the cantilever tip. On the basis of this novel phenomenon, small-sized surface relief gratings (SRG)s and their alignment were fabricated and observed by current-sensing atomic force microscopy. The rate of mass transport for the polymer is mainly controlled by the applied time at constant voltage bias between the cantilever and the electrode/substrate.

The manipulation of mass transport and orientation of azobenzene molecules have been of considerable interest in optoelectronic devices such as data storage memory devices. As one of the more promising applications, many studies on surface relief gratings (SRGs), which can be created by two interfering beams, have been reported with azo-polymers.¹ The underlying mechanism is based on trans–cis isomerization cycles of azobenzene molecules. These isomerization cycles and the interaction of the optical field induces motion on the azobenzene molecules and their realignment. The dimensions of the gratings are wavelength-dependent (laser used). Scanning near-field optical microscopy (SNOM) has also been used for azobenzene patterning for high-density memory devices in order to overcome the spatial resolution limited by the wavelength of the laser beam.² A line width at the 100-nm scale was optically inscribed and read by SNOM with polarization control. Thermally induced mass transport patterns of azobenzene polymers have also been reported using pulsed laser irradiation.³ This was carried out based on the thermal cis–trans back-isomerization of azobenzene molecules after pulsed irradiation. The form of the decay curves and reorientation of the molecules depended on the pulse energy.

On the other hand, external electric-field-induced alignment of azobenzene molecules is of interest in molecular manipulation and nonlinear optical (NLO) applications.⁴ Recently, this phenomenon has been utilized to fabricate a complex structure of $\chi^{(2)}$ gratings.⁵ This could be done with a high-electric-field poling or direct corona electrical poling of azobenzene polymer films before or after the fabrication of the SRGs. The fundamental study on the electric-field-induced dipole alignment of azobenzene polymers has been recently investigated.⁶ Furthermore, the manipulation of azobenzene single molecules has also been reported using scanning tunneling microscopy (STM). The azobenzene single molecule changed its orientation (state) and

was made mobile on an Au(111) surface by applying an external electric field.⁷ The phase shift switching of a single azobenzene molecule between cis and trans form was also controlled by using an external electric field and current flow with STM.⁸ These observations opened up the possibility of electro-nanolithography of azobenzene films with other surface probe microscopy (SPM) techniques.

In this work, we report the nanomanipulation and electro-nanopatterning of azobenzene polymer LbL ultrathin film,⁹ which is a dielectric material with high dipole moment from the azo-chromophore, using AFM electrical-field-induced nanolithography. The control of nanodot arrays on the LbL films is first shown. Then, the electric-field-induced mass transport properties of the azobenzene molecules were investigated. This is achieved by using a contact mode current-sensing AFM which locally applies an electric field and aligns the azobenzene polymer with current flow between the AFM cantilever and electrode, followed by scanning the cantilever. Using this setup, the formation of small-sized wavelength-independent surface relief gratings of azobenzene polymer LbL ultrathin film was observed. Since the dipole moment of the azo chromophore can be aligned by the external electric field, the inscribed surface gratings are expected to give a spatially modulated birefringence which could provide significant refractive index modulation at the microscale to nanoscale.

To investigate the possibility of nanometer-scale manipulation, we have utilized poly{1–4[4-(3-carboxy-4-hydroxyphenylazo) benzenesulfonamido]-1,2-ethanediylsodium salt} (PAZO) and poly(diallyldimethylammonium chloride) (PDADMAC) films prepared using the electrostatic LbL deposition technique.¹⁰ The LbL self-assembly method, initially reported by Decher et al., is one of the most convenient techniques for fabricating molecularly controlled ultrathin multilayer films.¹¹

PAZO and PDADMAC were both commercially available from Aldrich and used without further purification. 3-Mercapto-

[†] Current address: National Center for Nanomaterials Technology, Pohang University of Science and Technology, Pohang, Korea 790-784.

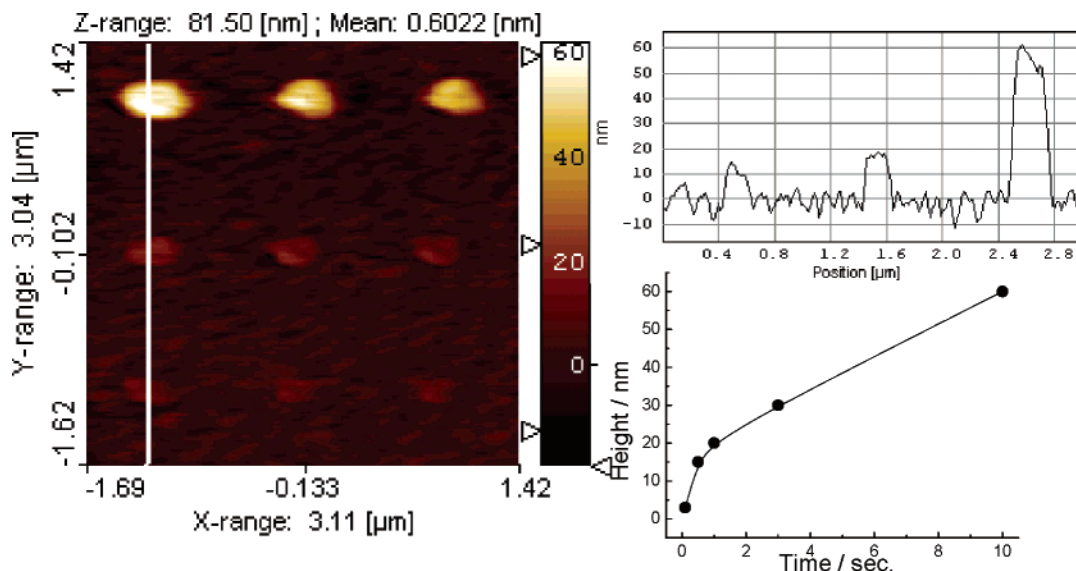


Figure 1. Nanodots array topographic image, height profile, and the change in height as a function of time.

1-propanesulfonic sodium for functionalization of the gold surface was also purchased from Aldrich.

The gold film with a thickness of ca. 50 nm was deposited by vacuum evaporation onto a BK7 glass slide with a 1–2-nm-thick chromium adhesion layer. The gold surface of the flat solid substrate was functionalized by immersing the slide for 1 h in an ethanol solution of 3-mercaptopropylsulfonic sodium salt (1 mM) (followed by rinsing), creating a uniformly charged (negative) substrate surface. The Au/Cr/glass with the functionalized surfaces was then alternately immersed for 15 min in aqueous solutions of the polycation and polyanion layer-by-layer until the desired number of layers was achieved. Rinsing with deionized water at pH 5.6 (Milli-Q, 18 M Ω) was done between depositions. Aqueous solutions of the PDADMAC and PAZO were prepared at a concentration of 1 mg/mL.

All electrowriting/nanopatterning experiments were done with a commercial current-sensing atomic force microscopy (CS-AFM) (PicoScan system or PicoPlus system, Molecular Imaging, Arizona) and Pt-coated cantilever tip. A positive electric field is defined when the Au surface is positively biased, and a negative electric field when the Au surface is negatively biased. The experiments were conducted under ambient conditions at \sim 50% relative humidity and 22 $^{\circ}$ C. Subsequent imaging after patterning was performed under the same conditions. The detail of the nanowriting experiments has been previously documented.¹²

The evaporated gold film (\sim 50 nm) on BK7 glass/Cr was used as the bottom electrode. The Pt/Ir-coated cantilever was brought into contact (\sim 0.5 nN) with the LbL film surface under ambient conditions. Figure 1 shows the nanodot arrays in the 10 bilayers of PAZO/PDADMAC layer-by-layer films ($d \approx$ 30 nm). The dots were fabricated by applying the bias voltage at 10 V (\sim 10⁸ V/m) for 0.5 s, 1 s, and 10 s. In the case of PDADMAC/poly(sodium,4-styrenesulfonate) (PSS) layer-by-layer films, no pattern was observed under the same conditions, confirming that the nanodot arrays originated from the presence of azobenzene groups in the PAZO layers. The size of the dots can be controlled by the residence time of the applied bias voltages (residence time of the cantilever tip on the substrate with bias voltage). The diameter of the dots is between 150 and 300 nm. The height change is also shown as a function of time of the applied voltage. As can be seen in this figure, the change in height is up to about 200%. This value is much larger

than the value reported using a joule heating patterning with PS thin films¹³ or cross-linking of the precursor polymers, i.e., in the absence of azobenzene chromophores.¹⁴ The mechanism of this property is not clear yet, but one possibility is that the applied electric field aligns the azo chromophore to the direction parallel to the axis between the cantilever and the electrode or perpendicular to the substrate. In fact, Rodriguez and co-workers have shown in a polarized absorption spectra that the dipoles of azo chromophores tend to orient in the direction of applied electric field, \sim 10⁸ V/m.^{4,5} Another possible mechanism of the dot fabrication is the softening the polymers to the glass transition temperature, T_g , due to joule heating. Lyuksyutov and co-workers have reported nanopatterning based on local joule heating with a conducting AFM cantilever.¹³ Current flow through the polymer film between cantilever and electrode resulted in local joule heating of the polymer surface above the T_g followed by electrostatic interaction of the softened polymer. Therefore, this large morphological change is possibly due to both the joule heating and electric-field-induced motion of the azobenzene molecule. This is not unreasonable, as the formation of microscopic surface relief gratings due to heat-induced mass transport with holographic methods is well-known.³

To investigate this effect further, we have applied an electric field to the PAZO/PDADMAC LbL films while scanning the cantilever over the patterned areas. Figure 2a shows the in situ patterning images, i.e., topographic and friction images during the scanning at a scan rate of 290 μ m/s at 10 V. The scanning direction for the pattern are also shown in this figure. The input current exceeded 10 nA, which can cause joule heating between cantilever and electrode. In the topographic image, the raised morphology was observed during the application of this bias voltage. Interestingly, the morphology kept changing even after turning the bias voltage off (0 V), and then, the raised morphology decayed gradually. The change in the friction image in the lateral direction was more than twice the length of the applied bias area. This change stopped when the raised morphological change completely decayed. More interestingly, a large mass transport was observed in the lateral direction after the patterning. Figure 2b shows the morphological and friction images observed at 0 V after writing. As indicated in this figure, the change of edge-to-edge distance is from 600 nm (during) to 850 nm (after) by the application of a 10 V bias. The mass transport is expected to be from the position of 0.25 μ m to 0.5

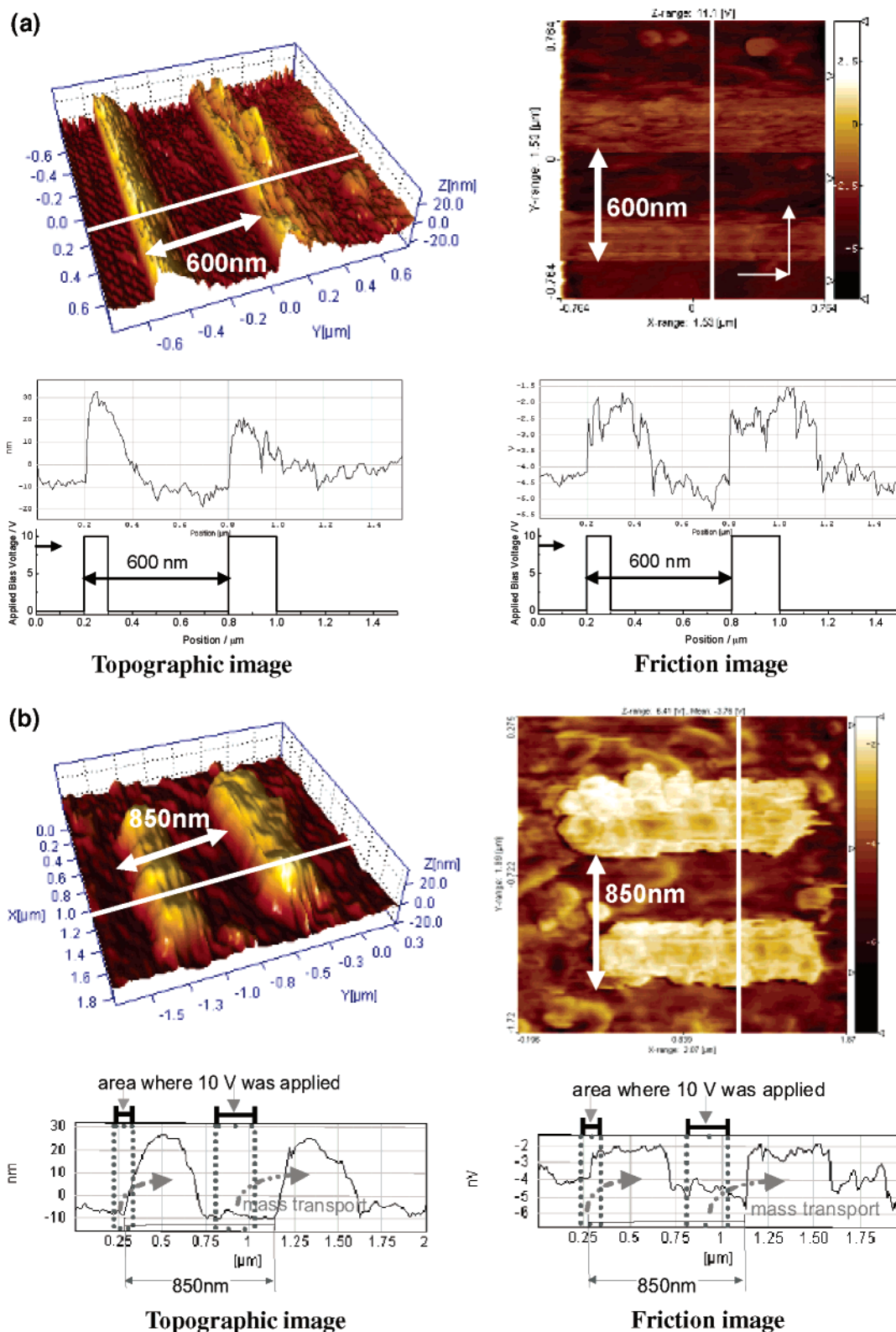


Figure 2. (a) Topographic and friction images and their height and applied voltage profiles during patterning at 10 V and 0 V. (b) Topographic and friction images and their profiles after patterning.

μm and from $0.85 \mu\text{m}$ to $1.35 \mu\text{m}$, as shown in the profile. The change in friction was almost the same value (5 nV) during and after scanning at 10 V. The height of the raised morphology was also about the same value (30–40 nm) during and after scanning at 10 V, indicating that the mass was initially raised and then transported to the lateral direction. This is schematically shown in Figure 3.

Since such a large mass transport in the lateral direction was not observed during the writing at 10 V, the mass transport should be a relatively slow process. McGee and co-workers reported the relaxation of electric-field-induced birefringes of an azobenzene polymer in a sandwiched cell to be between 20 and 100 s,^{6b} confirming that the reorientation of the dipole is indeed a slow process. It also should be noted that Tripathy

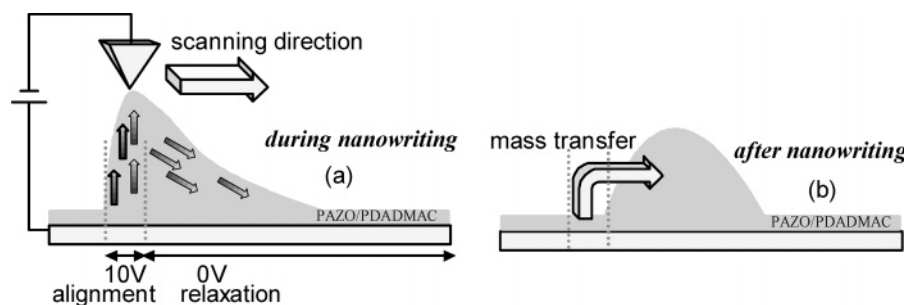


Figure 3. Schematic diagram of mass transfer effect.

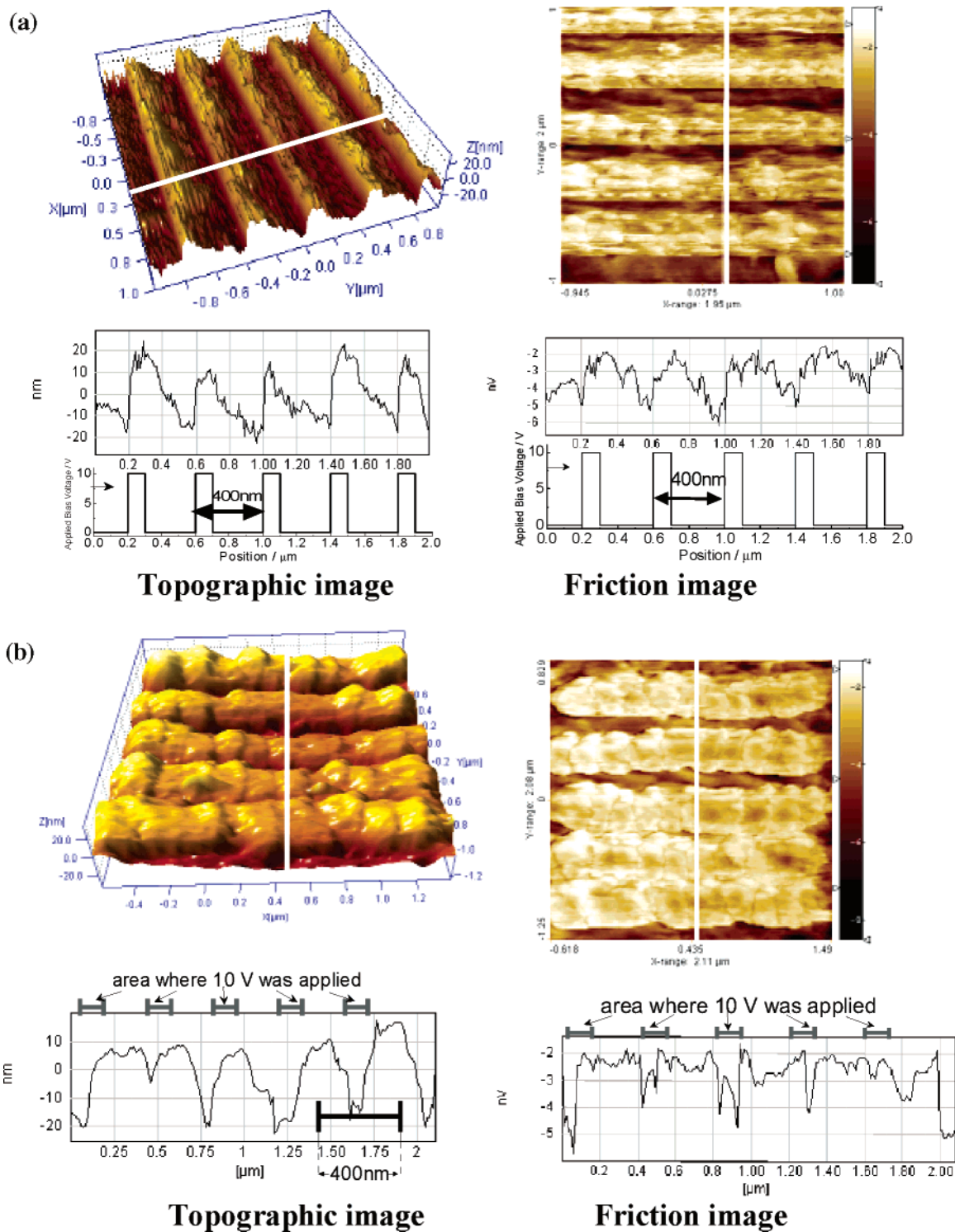


Figure 4. (a) Topographic and friction images and their height and applied voltage profiles during patterning at 10 V and 0 V. (b). Topographic and friction images and their profiles after patterning.

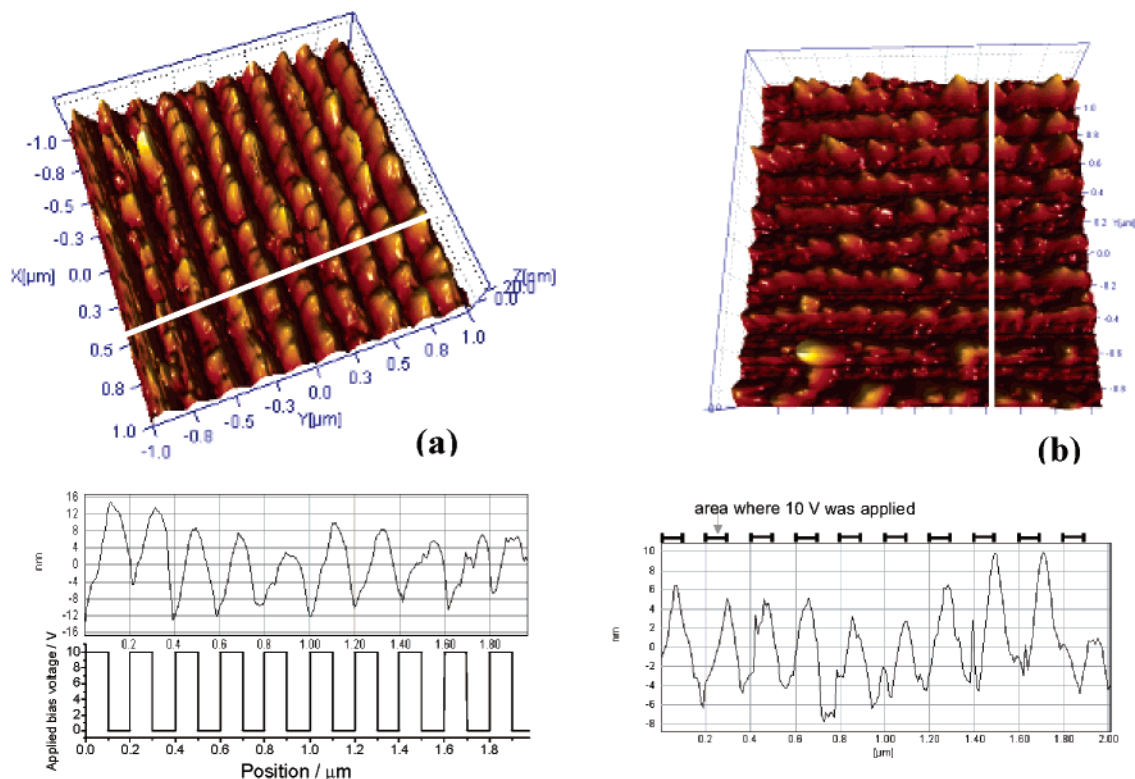


Figure 5. Topographic images during (a) and after (b) electrowriting of small gratings.

and co-workers have reported in SRG experiments (laser used) using azobenzene LbL ultrathin films that the inert polymers could be dragged along with the azobenzenes due to the electrostatic interaction between polyelectrolytes and azobenzene dyes.¹⁵ A possible mechanism is as follows: First, the PAZO is softened to T_g by joule heating and then aligned to the direction of the moving electric field. The softened azobenzene is then realigned to the direction of the moving cantilever tip, so that the mass transfer was observed in this direction. After turning the bias voltage off, the residual heating of the cantilever induced the direction of relaxation of the azobenzene polymer. Indeed, the domains or alignment of the PAZO/PDADMAC film was observed after patterning as shown in Figure 2b. In the same experiments using PAZO/poly(allylamine hydrochloride) (PAH), the obvious mass transport was not observed, indicating that the electrostatic molecular interaction with the counter polyelectrolyte has an important role in the azobenzene mass transport mechanism. This result corresponds to previous SRGs (laser used) experiments reported by other groups.^{15b,c}

On the basis of this mass transfer property, an electric-field-induced grating was fabricated as shown in Figure 4a (during fabrication) and b (after fabrication). For the fabrication of the gratings, the cantilever was scanned at $290 \mu\text{m/s}$ alternately at 0 V and at 10 V. Again, morphological and friction changes were observed even after the bias voltage was turned off. As can be seen in Figure 4a, after each application of a 10 V bias, the change in the morphology was almost completely decayed. In this case, the mass transfer to the lateral direction was observed within the area before another 10 V was applied. However, mass transport in the lateral direction was observed if another voltage was not applied (Figure 2). This indicates that the application of another 10 V to hold back further mass transport and start another mass transport (at the points of 0.6, 1.0, 1.4, and 1.6 μm in Figure 4a) was necessary in order to form a regular pattern. In this figure, the height is about 25–35 nm, and the grating spacing is about 400 nm. These values

are about the same during (Figure 4a) and after (Figure 4b) the patterning. The peak positions of the gratings are moved into the center between the valleys. Since the mass transport was observed within the area, the border was not clearly observed in friction images, while it was clearly seen during the writing stage. Furthermore, some domains are clearly observed in the friction image after the relaxation.

Smaller-sized gratings were also fabricated as shown in Figure 5. In this case, the height change was about 12–20 nm, which is much less than the value observed in Figures 2–4. This was possible since the alternating 10 V bias was applied before the relaxation was completed. As can be seen in this figure, the gratings were formed in a more orderly line. It should be noted that the spacing is about 200 nm, which is smaller than the limit of conventional SRGs created by argon ion laser interferences in holographic methods, i.e., wavelength-independent. The height change after scanning at 10 V was in about the same range as during the patterning stage (10 V). Since 10 V was applied in small spacings, the mass transport in the lateral direction was not observed as in previous cases, although some domain formation was observed. Again, this shows that the application of another 10 V to hold back further mass transport was critical. This indicates that the mass transport can be controlled by the timing (alternation) or range of bias voltages in electro-nanopatterning.

In summary, we have demonstrated electro-nanopatterning in azobenzene LbL ultrathin films. Arrays of nanodots were created by a local electric field and joule heating. Mass transport and alignment of azobenzene were observed by scanning the cantilever after heating the sample with the cantilever. The rate of mass transport of azobenzene is mainly controlled by the residence time of the applied voltages between the cantilever and the electrode. Moreover, on the basis of this novel phenomenon, small-sized gratings can be fabricated by electro-nanopatterning with current-sensing atomic force microscopy. The demonstrated method should provide new opportunities for

both fundamental studies of electropatterns and for nanoscale device applications using azobenzene polymer ultrathin films. Further studies are underway on study of the mechanism and the precise manipulation of mass transport under controlled humidity conditions, temperature, or using other thickness.

Acknowledgment. The authors would like to acknowledge support from various funding agencies that made this work possible: DMR-06-02896, DMR-05-04435, instrument support from DMR-03-15565, technical support from Molecular Imaging (Agilent Technologies), and Robert Welch Foundation, E-1551.

Supporting Information Available: In situ surface plasmon monitoring of the layer-by-layer build-up of PAZO and PDAD-MAC. This material is available free of charge via the Internet at <http://pubs.acs.org>.

References and Notes

- (1) (a) Batalla, E.; Natansohn, A. L.; Rochon, P. L. *Appl. Phys. Lett.* **1995**, *66*, 136. (b) Kim, D. Y.; Tripathy, S. K.; Li, L.; Kumar, J. *Appl. Phys. Lett.* **1995**, *66*, 1166. (c) Fukuda, T.; Matsuda, H.; Shiraga, T.; Kimura, T.; Kato, M.; Viswanathan, N. K.; Kumar, J.; Tripathy, S. K. *Macromolecules* **2000**, *33*, 4220. (d) Natansohn, A.; Rochon, P. *Chem. Rev.* **2002**, *102*, 4139.
- (2) (a) Karageorgiev, P.; Neher, D.; Schulz, B.; Stiller, B.; Pietsch, U.; Giersig, M.; Brehmer, L. *Nat. Mater.* **2005**, *4*, 699. (b) Likodimos, V.; Labardi, M.; Pardi, L.; Allegrini, M.; Giordano, M.; Arena, A.; Patane, S. *Appl. Phys. Lett.* **2003**, *82*, 3313.
- (3) (a) Leopold, A.; Wolff, J.; Baldus, O.; Huber, H.; Bieringer, T.; Zilker, S. J. *J. Chem. Phys.* **2000**, *113*, 833. (b) Geon, J. L.; Oh, C. H.; Lee, Y. P.; Kang, I. A.; Han, Y. K. *J. Appl. Phys.* **2005**, *97*, 093101. (c) Rodríguez, F. J.; Sánchez, C.; Villacampa, B.; Alcalá, R.; Cases, R.; Millaruelo, M.; Oriol, L. *Appl. Phys. Lett.* **2005**, *87*, 201914.
- (4) (a) Rodríguez, V.; Adamietz, F.; Sanguinet, L.; Buffetau, T.; Sourisseau, C. *J. Phys. Chem. B* **2003**, *107*, 9736. (b) Ribeiro, P. A.; Balogh, D. T.; Giacometti, J. A. *IEEE Trans. Dielectr. Electr. Insul.* **2000**, *7*, 572.
- (5) (a) Lagugné-Labarthe, F.; Bruneel, J. L.; Rodriguez, V.; Sourisseau, C. *J. Phys. Chem. B* **2004**, *108*, 1267. (b) Schaller, R. D.; Saykally, R. J.; Shen, Y. R.; Lagugné-Labarthe, F. *Opt. Lett.* **2003**, *28*, 1296. (c) Chang, H. J.; Kang, B.; Choi, H.; Wu, J. W. *Opt. Lett.* **2005**, *30*, 183.
- (6) (a) Campbell, V. E.; In, I.; McGee, D. J.; Woodward, N.; Caruso, A.; Gopalan, P. *Macromolecules* **2006**, *39*, 957. (b) McGee, D. J.; Fukunaga, J. Y.; Zielinski, T.; Yang, M.; Salter, C. *J. Appl. Phys.* **2005**, *97*, 103102.
- (7) Comstock, M. J.; Cho, J.; Kirakosian, A.; Crommie, M. F. *Phys. Rev. B* **2005**, *72*, 153414.
- (8) Yasuda, S.; Nakamura, T.; Matsumoto, M.; Shigekawa, H. *J. Am. Chem. Soc.* **2003**, *125*, 16430.
- (9) (a) Advincula, R.; Park, M.-K.; Baba, A.; Kaneko, F. *Langmuir* **2003**, *19*, 654. (b) Shinbo, K.; Baba, A.; Kaneko, F.; Kato, T.; Kato, K.; Advincula, R.; Knoll, W. *Mater. Sci. Eng. C* **2002**, *22*, 319. (c) Shinbo, K.; Ishikawa, J.; Baba, A.; Kato, K.; Kaneko, F.; Advincula, R. *Jpn. J. Appl. Phys.* **2002**, *41*, 2753. (d) Kaneko, F.; Kato, T.; Baba, A.; Shinbo, K.; Kato, K.; Advincula, R. *Colloids Surf., A* **2002**, *805*, 198. (e) Park, M.-K.; Advincula, R. *Langmuir* **2002**, *18*, 4532.
- (10) Dante, S.; Advincula, R.; Frank, C. W.; Stroeve, P. *Langmuir* **1999**, *15*, 193.
- (11) Decher, G.; Hong, J. D. *Makromol. Chem. Makromol. Symp.* **1991**, *46*, 321.
- (12) Baba, A.; Locklin, J.; Xu, R.; Advincula, R. *J. Phys. Chem. B* **2006**, *110*, 42.
- (13) (a) Lyuksyutov, S. F.; Vaia, R. A.; Paramonov, P. B.; Juhl, S.; Waterhouse, L.; Ralich, R. M.; Sigalov, G.; Sancaktar, E. *Nat. Mater.* **2003**, *2*, 468. (b) Lyuksyutov, S. F.; Paramonov, P. B.; Juhl, S.; Vaia, R. A. *Appl. Phys. Lett.* **2003**, *83*, 4405. (c) Juhl, S.; Phillips, D.; Vaia, R. A.; Lyuksyutov, S. F.; Paramonov, P. B. *Appl. Phys. Lett.* **2004**, *85*, 1.
- (14) (a) Jegadesan, S.; Advincula, R. C.; Valiyaveetil, S. *Adv. Mater.* **2005**, *17*, 1282. (b) Jang, S.-Y.; Mearquez, M.; Sotzing, G. A. *J. Am. Chem. Soc.* **2004**, *126*, 9476. (c) Schneegans, O.; Moradpour, A.; Houze, F.; Angelova, A.; Villeneuve, C. H.; Allongue, P.; Chretien, P. *J. Am. Chem. Soc.* **2001**, *123*, 11486. (c) Jegadesan, S.; Sindhu, S.; Advincula, R. C.; Valiyaveetil, S. *Langmuir* **2006**, *22*, 780.
- (15) (a) Lee, S.-H.; Balasubramanian, S.; Kim, D. Y.; Viswanathan, N. K.; Bian, S.; Kumar, J.; Tripathy, S. K. *Macromolecules* **2000**, *33*, 6534. (b) He, J.-A.; Bian, S.; Li, L.; Kumar, J.; Tripathy, S. K.; Samuelson, L. A. *Appl. Phys. Lett.* **2000**, *76*, 22. (c) He, J.-A.; Bian, S.; Li, L.; Kumar, J.; Tripathy, S. K.; Samuelson, L. A. *J. Phys. Chem. B* **2000**, *104*, 10513.